The current issue and full text archive of this journal is available at
www.emeraldinsight.com/0264-4401.htm

Received 19 April 2010
Revised 27 November 2010,
18 March 2011,
26 May 2011
Accepted 9 June 2011

Multimodal method for linear liquid sloshing in a rigid tapered conical tank

Ivan Gavrilyuk
University of Cooperative Education, Eisenach, Germany
Marten Hermann
Friedrich-Schiller-Universitat Jena, Jena, Germany
Ivan Lukovsky and Oleksandr Solodun
Institute of Mathematics, National Academy of Sciences of Ukraine, Kiev, Ukraine, and
Alexander Timokha
CeSOS, Norwegian University of Science and Technology, Trondheim, Norway and
Institute of Mathematics, National Academy of Sciences of Ukraine, Kiev, Ukraine

Abstract

Purpose – The purpose of this paper is to derive linear modal equations describing the forced liquid sloshing in a rigid truncated (tapered) conical tank, as well as to show how to couple these modal equations with "global" dynamic equations of a complex mechanical system carrying this tank.

Design/methodology/approach – Derivation of the modal equations can be based on the Trefftz variational method developed by the authors in a previous paper. Describing the coupled dynamics utilizes Lukovsky' formulas for the resulting hydrodynamic force and moment due to liquid sloshing.

Findings – The so-called Stokes-Joukowski potentials can be found by using the Trefftz method from the authors' previous paper with the same polynomial-type functional basis. Coupling the modal equations with the global dynamic equations becomes a relatively simple task facilitated by Lukovsky's formulas. Using the linear multimodal method can be an efficient alternative to traditional numerical and analytical tools employed for studying the coupled vibrations of a tower with a conical rigid tank on the tower top.

Practical implications – The derived modal equations are equipped by tables with the computed non-dimensional hydrodynamic coefficients. Interested readers (engineers) can incorporate the modal equations into the global dynamic equations of a whole mechanical system without new computations of these coefficients.

Originality/value – The multimodal method can be an alternative to traditional numerical tools. Using the derived modal equations simplifies analytical studies and provides efficient calculations of the coupled dynamics of a mechanical system carrying a rigid tapered conical tank with a liquid.

Keywords Liquids, Flow, Hydrodynamics, Sloshing, Conical tank, Modal equations, Coupled dynamics

Paper type Research paper

Engineering Computations: International Journal for Computer-Aided Engineering and Software
Vol. 29 No. 2, 2012
pp. 198-220

0264-4401
DOI 10.1108/02644401211206052

The authors thank the German Research Society (DFG) for financial support (project DFG 436UKR 113/33/00).

1. Introduction

Water towers and offshore platforms are examples of engineering constructions dealing with the coupled "global" dynamics of mechanical systems containing a tapered conical tank partly filled with a liquid. Describing this dynamics (see, fundamentals in the books by Morand and Ohayon (1995) and Faltinsen and Timokha (2009)) is typically carried out by using either the computational fluid dynamics (CFD) or the so-called equivalent mechanical system. The latter implies that hydrodynamic loads due to sloshing are related to inertial forces and moments generated by a fictitious mass-spring (or pendulum) system "installed" in the tank instead of the contained liquid. The equivalent mechanical systems require experimental (Dokuchaev, 1964; Mikishev and Dorozhkin, 1961; Bauer, 1982; El Damatty *et al.*, 2000; Casciati *et al.*, 2003) and theoretical data on the natural sloshing frequencies and modes. Examples of those systems can be found in the papers by El Damatty and Sweedan (2006), Dutta *et al.* (2004) and Sweedan (2009). An alternative could be multimodal methods which reduce the original free-boundary problem to a system of ordinary differential equations (ODEs), the so-called modal equations, coupling the generalized coordinates responsible for instant displacements of the natural sloshing modes. Fundamentals of the multimodal methods are outlined by Lukovsky (1990) and Faltinsen and Timokha (2009) and, in some detail for conical tanks, by Gavrilyuk *et al.* (2005).

Describing the coupled dynamics of a complex mechanical system carrying a tank with a liquid requires an accurate prediction of hydrodynamic loads which (see, discussion on Faltinsen and Timokha (2009, pp. 9-10)) can be classified as either "impact" (impulsive) or "dynamic" (non-impulsive). "Dynamic" loads are characterized by dominant time variations on the time scale of the highest sloshing period which is typically of the order 1 s, but "impact" loads last from about 10^{-3} to 10^{-2} s. The "impact" loads may cause hydroelastic slamming (Chapter 11 by Faltinsen and Timokha (2009)). Coupling global dynamics and sloshing requires the resulting hydrodynamic (sloshing) force and moment which are, in fact, integrals of the hydrodynamic pressure over the wetted tank surface. The resulting hydrodynamic force and moment are basically determined by "dynamic" sloshing loads. Hydroelastic tank vibrations caused by sloshing matter when structural reaction in terms of deflections and stresses cannot be decoupled with "dynamic" loads. Within the framework of linear analysis, this decoupling is possible when the elastic tank vibrations have the eigenfrequencies that are much higher than the lowest natural sloshing frequencies. The present study assumes this decoupling and, therefore, focuses on the rigid tank. Interested readers can find details on eigen- and forced elastic vibrations of conical tanks in the papers by El Damatty *et al.* (2005), El Damatty and Sweedan (2006) and Sweedan (2009). A particular task of these and similar papers is description of hydrodynamic pressure loads. Even though the resulting hydrodynamic force and moment are integrals of the pressure loads over the wetted tank surface, we can avoid calculation of the pressure field by employing the Lukovsky formulas (Lukovsky, 1990; Lukovsky and Timokha, 1995; Faltinsen and Timokha, 2009, Chapters 5 and 7).

The multimodal methods are well elaborated for linear sloshing in rigid tanks (see, a modern description of the linear multimodal methods in Chapter 5 by Faltinsen and Timokha (2009)). Deriving the corresponding linear modal equations requires the natural sloshing modes and the so-called Stokes-Joukowski potentials whose exact analytical expressions exist for upright cylindrical tanks of rectangular, circular or sectoral base. The tapered (truncated) conical tank belongs to geometric shapes for which the literature does not give the analytical natural sloshing modes and the Stokes-Joukowski potentials.

Approximate natural sloshing modes for a truncated conical tank were constructed by Gavrilyuk *et al.* (2008) by using the Trefftz method. In the present paper, we employ the same Trefftz variational method to get an approximation of the Stokes-Joukowski potentials and, using these potentials and the approximate natural sloshing modes, derive the required linear modal equations. The linear modal equations provide a semi-analytical description of liquid sloshing in tapered conical tanks. Solutions of these equations make it possible to compute the resulting hydrodynamic force and moment. The latter force and moment are needed for coupling the modal equations and the dynamic equations of tank-carrying structures.

The introductory Section 2 presents necessary elements of the linear multimodal method for an axisymmetric tank. Interested readers can find more details in Chapter 5 by Faltinsen and Timokha (2009). The method reduces description of the linear liquid sloshing to a set of the ODEs responsible for small-magnitude displacements of the natural sloshing modes. The displacements are associated with nonzero generalized coordinates. In Section 3, we extend the Trefftz variational method by Gavrilyuk *et al.* (2008) for computing the natural sloshing modes and the Stokes-Joukowski potentials. Using the constructed Trefftz solutions makes it possible to get numerical values of the hydrodynamic coefficients appearing in the modal equations as well as in expressions for the resulting hydrodynamic force and moment. The hydrodynamic coefficients are tabled to facilitate implementation of the derived linear modal equations by practically oriented readers. Two examples on how to use the modal equations for the coupled dynamics are presented in Section 4.

2. Multimodal method

1. Boundary value problem on linear liquid sloshing

We consider a rigid tank of conical shape (frustum of cone) partially filled by an ideal incompressible liquid with irrotational flow. The cone has the semiapex angle θ_0. When the tank does not move, the symmetry axis is parallel to the gravity acceleration vector. Figure 1 shows geometric notations where, as we see, S_1 is the wetted tank wall, S_2 is the tank bottom, and Σ_0 is the unperturbed (mean) free surface. Liquid motions are considered in the $Oxyz$-coordinate system rigidly fixed with the tank so that the origin is superposed with the geometric center of Σ_0, and Ox is directed upwards along the symmetry axis. It is implicitly assumed that the tank can be a component of a complex mechanical system which, in addition, consists of solid and elastic elements. The system performs coupled small-amplitude motions so that sloshing can be described within the framework of the linear sloshing theory. The resulting hydrodynamic force and moment due to sloshing appear as a hydrodynamic response to these small-amplitude tank motions.

The oscillatory tank motions are considered with respect to an inertial coordinate system rigidly fixed with the Earth. They are characterized by six degrees of freedom and can be described by the translational velocity vector $\mathbf{v}_0(t) = (\dot{\eta}_1, \dot{\eta}_2, \dot{\eta}_3)$, and the instantaneous angular velocity vector $\boldsymbol{\omega}(t) = (\dot{\eta}_4, \dot{\eta}_5, \dot{\eta}_6)$. In the tank-fixed coordinate system $Oxyz$, the linearized projections of the gravity acceleration vector take the form $\mathbf{g} = (g_1, g_2, g_3) = (-g, g\eta_6, -g\eta_5)$.

We introduce the absolute velocity potential $\Phi(x, y, z, t)$ and function $\xi(y, z, t)$ determining the small vertical free-surface elevations. The functions Φ and ξ can be found from the following boundary value problem (Lukovsky *et al.*, 1984; Faltinsen and Timokha, 2009):

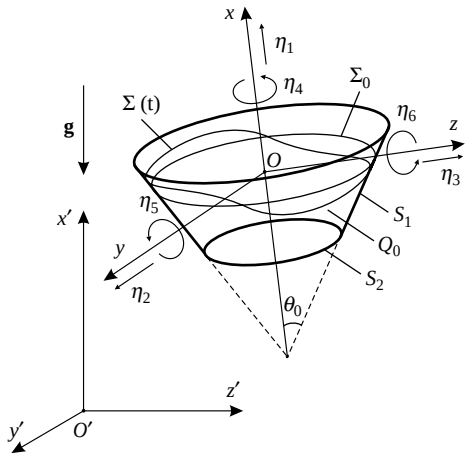

Notes: Three-dimensional view of the tank performing small-amplitude oscillatory motions associated with six degrees of freedom, $\eta_i, i = 1, \ldots, 6$

Figure 1.
A tapered rigid conical tank partially filled with a liquid

$$\nabla^2\Phi = 0 \quad \text{in} \quad Q_0, \tag{1}$$

$$\frac{\partial\Phi}{\partial n} = \mathrm{v}_0 \cdot \mathbf{n} + \boldsymbol{\omega} \cdot (\mathbf{r} \times \mathbf{n}) \quad \text{on} \quad S_0, \tag{2}$$

$$\frac{\partial\Phi}{\partial n} = \mathbf{v}_0 \cdot \mathbf{n} + \boldsymbol{\omega} \cdot (\mathbf{r} \times \mathbf{n}) - \frac{\partial\xi}{\partial t} \quad \text{on} \quad \Sigma_0, \tag{3}$$

$$\frac{\partial\Phi}{\partial t} - \mathbf{g} \cdot \mathbf{r} = 0 \quad \text{on} \quad \Sigma_0, \tag{4}$$

$$\int_{\Sigma_0} \xi d\boldsymbol{S} = 0, \tag{5}$$

where $S_0 = S_1 \cup S_2$ is the mean wetted tank surface, $\mathbf{n}$ is the outer normal vector, and $\mathbf{r} = (x, y, z)$.

The boundary value problem (1) needs the following initial conditions that define the initial free-surface shape and normal velocities:

$$\xi(y, z, t_0) = \xi_0(y, z), \quad \left.\frac{\partial\Phi}{\partial n}\right|_{\Sigma(t_0)} = \Phi_0(x, y, z). \tag{6}$$

When we look for a steady-state regime occurring due to the T-periodic tank motion, the periodicity conditions:

$$\xi(y, z, t + T) = \xi(y, z, t), \quad \nabla\Phi(x, y, z, t + T) = \nabla\Phi(x, y, z, t) \tag{7}$$

should be adopted instead of the initial conditions (6).

2. Modal equations for axisymmetric tanks

For axisymmetric containers, one can use the cylindrical coordinate system, $x = x,\ y = r\cos\theta,\ z = r\sin\theta$, and separate the angular variable θ in the original boundary value problem (1). The geometric notations are shown in Figure 2 by the meridional cross-section and the plan view of the mean liquid domain. Furthermore, the linear multimodal method assumes the following modal solution (Faltinsen and Timokha, 2009, Chapter 5):

$$\xi(r,\theta,t) = \sum_{m=0}^{\infty}\sum_{i=1}^{\infty}\left(\beta^{c}_{m,i}(t)\cos(m\theta) + \beta^{s}_{m,i}(t)\sin(m\theta)\right)\xi_i(r) \tag{8}$$

($\xi_i(r) = \phi_i^{(m)}(0,r)$), and:

$$\begin{aligned}\Phi(x,r,\theta,t) =& \mathbf{v}_0(t)\cdot\mathbf{r} + \omega(t)\cdot\Omega_0(x,r,\theta)\\ &+\sum_{m=0}^{\infty}\sum_{i=1}^{\infty}\left(R^{c}_{m,i}(t)\cos(m\theta) + R^{s}_{m,i}(t)\sin(m\theta)\right)\phi_i^{(m)}(x,r).\end{aligned} \tag{9}$$

Here, $\beta^{c}_{m,i}, \beta^{s}_{m,i}, R^{c}_{m,i}$ and $R^{s}_{m,i}$ are the generalized coordinates, $\mathbf{r} = (x,y,z)$, and:

$$\phi_{m,i,1} = \phi_i^{(m)}(x,r)\cos(m\theta), \quad \phi_{m,i,2} = \phi_i^{(m)}(x,r)\sin(m\theta) \tag{10}$$

are the natural sloshing modes which are eigenfunctions of the spectral boundary problem:

$$\nabla^2\phi = 0, \quad \mathbf{r}\in Q_0; \quad \frac{\partial\phi}{\partial n} = 0, \quad \mathbf{r}\in S_0; \quad \frac{\partial\phi}{\partial n} = \kappa\phi, \quad \mathbf{r}\in\Sigma_0; \quad \int_{\Sigma_0}\phi dS = 0. \tag{11}$$

Specifically for the axisymmetric tanks and $m \geq 1$, there are two conjugate eigenfunctions $\phi_{m,i,1}$ and $\phi_{m,i,2}$ corresponding to the same eigenvalue $\kappa = \kappa_{m,i}$. These eigenvalues determine the natural sloshing frequencies by the formula (Morand and Ohayon, 1995; Faltinsen and Timokha, 2009):

$$\sigma_{m,i} = \sqrt{g\kappa_{m,i}}.$$

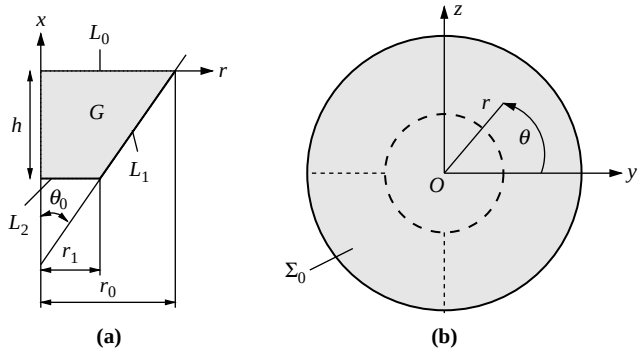

Figure 2.
The meridional cross-section (a) and the plan view (b) of the mean liquid domain

Note: Geometric notations

The three components of the harmonic vector-function $\Omega_0(x,y,z) = (\Omega_{01}, \Omega_{02}, \Omega_{03})$ are the so-called Stokes-Joukowski potentials $\Omega_{0i}, i = 1,2,3$ (Joukowski, 1885) which are determined by the following Neumann boundary value problem:

$$\nabla^2\Omega_0 = 0, \quad \mathbf{r} \in Q_0; \quad \frac{\partial\Omega_0}{\partial n} = \mathbf{r}\times\mathbf{n}, \quad \mathbf{r} \in S_0 + \Sigma_0. \tag{12}$$

The problem (12) admits separation of the angular variable θ so that:

$$\Omega_{01} = 0, \quad \Omega_{02} = \chi(x,r)\sin\theta, \quad \Omega_{03} = -\chi(x,r)\cos\theta, \tag{13}$$

where $\chi(x, r)$ is solution of the corresponding boundary value problem in the meridional cross-section G (Figure 1). For a tapered conical tank, function χ satisfies the following boundary value problem:

$$r^2\frac{\partial^2\chi}{\partial x^2} + r\frac{\partial\chi}{\partial r} + r^2\frac{\partial^2\chi}{\partial r^2} - \chi = 0 \quad \text{in} \quad G, \tag{14}$$

$$\frac{\partial\chi}{\partial x} = r \quad \text{on} \quad L_0(x=0), \tag{15}$$

$$\frac{\partial\chi}{\partial\nu} = -x\cos\theta_0 - r\sin\theta_0 \quad \text{on} \quad L_1(r = x\tan\theta_0 + r_0), \tag{16}$$

$$\frac{\partial\chi}{\partial x} = -r \quad \text{on} \quad L_2(x=-h), \tag{17}$$

where h is the liquid depth, and r_1 is the tank bottom radius (see notations in Figure 2).

The modal solutions (8) and (9) automatically satisfy the Laplace equation and the body-boundary condition of the boundary value problem (1). Substituting equations (8) and (9) into the kinematic boundary condition (3), and accounting for the orthogonality of the natural sloshing modes on Σ_0 gives:

$$\dot\beta^c_{m,i} = \kappa_{m,i}R^c_{m,i} \quad \text{and} \quad \dot\beta^s_{m,i} = \kappa_{m,i}R^s_{m,i}.$$

In addition, using the dynamic boundary condition (4) leads to the modal equations appearing as linear ODEs with respect to the generalized coordinates $\beta^c_{m,i}$ and $\beta^s_{m,i}$. For axisymmetric containers, there are only the following two independent sets of linear modal equations with a nonzero right-hand side:

$$\mu_i(\ddot\beta^c_i + \sigma_i^2\beta^c_i) = -\lambda_i(\ddot\eta_2 - g\eta_6) - \lambda_{0i}\ddot\eta_6, \tag{18}$$

$$\mu_i(\ddot\beta^s_i + \sigma_i^2\beta^s_i) = -\lambda_i(\ddot\eta_3 + g\eta_5) + \lambda_{0i}\ddot\eta_5, \tag{19}$$

which are responsible for sloshing in planes Oxy and Oxz, respectively, where:

$$\beta^c_i = \beta^c_{1,i}, \quad \beta^s_i = \beta^s_{1,i}.$$

The introduced hydrodynamic coefficients in equations (18) and (19) are:

$$\kappa_i = \kappa_{1,i}, \quad \sigma_i^2 = g\kappa_i = \sigma^2_{1,i}, \tag{20}$$

$$\mu_i = \frac{\rho\pi}{\kappa_{1,i}} \int_{L_0} r\left(\phi_i^{(1)}\right)^2 dr; \quad \lambda_i = \rho\pi \int_{L_0} r^2 \phi_i^{(1)} dr; \quad \lambda_{0i} = \rho\pi \int_{L_0} r^2 \chi \phi_i^{(1)} dr, \tag{21}$$

where L_0 is intersection of the mean free-surface Σ_0 and the meridional plane. For remaining generalized coordinates, one gets the homogeneous linear modal equations:

$$\ddot{\beta}^c_{m,i} + \sigma^2_{m,i}\beta^c_{m,i} = \ddot{\beta}^s_{m,i} + \sigma^2_{m,i}\beta^s_{m,i} = 0, \quad m \neq 1. \tag{22}$$

Having known the natural sloshing modes, and the Stokes-Joukowski potentials, one can immediately compute the hydrodynamic coefficients (19). Furthermore, the vertical free-surface elevation and velocity potential (multimodal solutions (8) and (9)) are determined by the generalized coordinates $\beta^c_{m,i}$ and $\beta^s_{m,i}$ to be found from the modal equations (17) and (22) by means of a time-step integration with the initial conditions:

$$\beta^c_{m,i}(0) = \left(\beta^c_{m,i}\right)_0, \beta^s_{m,i}(0) = \left(\beta^s_{m,i}\right)_0, \dot{\beta}^c_{m,i}(0) = \left(\beta^c_{m,i}\right)_1, \dot{\beta}^s_{m,i}(0) = \left(\beta^s_{m,i}\right)_1$$

associated with equation (6), or, alternatively, with the periodicity conditions following from equation (7).

For *non-prescribed tank motions* ($\eta_k(t)$, $k = 1, \ldots, 6$ are unknown), the linear modal equations (17) should be incorporated into the global dynamic equations of the tank-carrying structure in which the resulting hydrodynamic force and moment due to sloshing determine the hydrodynamic response. Because the modal solution (9) makes it possible to compute the hydrodynamic pressure by using the Bernoulli equation, we can find the resulting hydrodynamic force and moment as integrals of the hydrodynamic pressure over the wetted tank surface. However, we can avoid this integration by using the Lukovsky formulas which express the force and moment as functions of the generalized coordinates β^c_i, β^s_i and η_k ($k = 1 \ldots, 6$) (Lukovsky, 1990; Lukovsky and Timokha, 1995; Faltinsen and Timokha, 2009).

The linear hydrodynamic force by Lukovsky needs to know the mean liquid mass center in the *Oxyz*-system:

$$\mathbf{r}_{lC_0} = (x_{lC_0}, y_{lC_0}, z_{lC_0}) = \rho \int_{Q_0} \mathbf{r} dQ / M_l, \tag{23}$$

where M_l is the liquid mass and ρ in the liquid density. Accounting for the fact that $y_{lC_0} = z_{lC_0} = 0$ in the considered axisymmetric case, the resulting hydrodynamic force by the Lukovsky formula has the following projections on the *Oxyz*-axes:

$$F_1(t) = F_x(t) = M_l(-g - \ddot{\eta}_1), \tag{24}$$

$$F_2(t) = F_y(t) = M_l(-\ddot{\eta}_6 x_{lC_0} + [g\eta_6] - \ddot{\eta}_2) - \sum_{k=1}^{\infty} \ddot{\beta}^c_k \lambda_k, \tag{25}$$

$$F_3(t) = F_z(t) = M_l(\ddot{\eta}_5 x_{lC_0} - [g\eta_5] - \ddot{\eta}_3) - \sum_{k=1}^{\infty} \ddot{\beta}^s_k \lambda_k. \tag{26}$$

The linear components $[g\eta_6]$ and $[g\eta_5]$ vanish when we consider projections on the Earth-fixed coordinates.

The linearized Lukovsky formula for the hydrodynamic moment (with respect to O) involves the liquid inertia tensor $\mathbf{J}_0^1$:

$$J_{0ij}^1 = \rho \int_{S_0+\Sigma_0} \Omega_{0i} \frac{\partial \Omega_{0j}}{\partial n}\, dS$$

which has, for the case of axisymmetric tanks, the two nonzero elements:

$$J_{022}^1 = J_{033}^1 = J_0 = \rho\pi \int_L \chi \frac{\partial \chi}{\partial n}\, ds. \tag{27}$$

Here, $L = L_0 + L_1 + L_2$, so that L_0, L_1 and L_2 are intersections of the meridional plane with the mean free-surface Σ_0, the tank walls S_1 and the tank bottom S_2, respectively, (Figure 1).

Using the linearized Lukovsky formulas, we obtain $F_4 = M_{Ox} = 0$, and:

$$F_5(t) = M_{Oy}(t) = M_l x_{lC_0}(g\eta_5 + \ddot{\eta}_3) - J_0\ddot{\eta}_5 - \sum_{j=1}^{\infty}\left(-\lambda_{0j}\ddot{\beta}_j^s + g\lambda_j\beta_j^s\right), \tag{28}$$

$$F_6(t) = M_{Oz}(t) = M_l x_{lC_0}(g\eta_6 - \ddot{\eta}_2) - J_0\ddot{\eta}_6 - \sum_{j=1}^{\infty}\left(\lambda_{0j}\ddot{\beta}_j^c - g\lambda_j\beta_j^c\right). \tag{29}$$

The hydrodynamic moment relative to another point A can be computed as:

$$\mathbf{M}_A = \mathbf{r}_{AO} \times \mathbf{F} + \mathbf{M}_O, \tag{30}$$

where $\mathbf{F} = (F_1, F_2, F_3)$, $\mathbf{M}_O = (F_4, F_5, F_6)$, and $\mathbf{r}_{AO}$ is the radius vector of the origin O with respect to A.

3. Nondimensional hydrodynamic coefficients

The introduced hydrodynamic coefficients are functions of the characteristic tank dimension which is, henceforth, associated with the unperturbed free-surface radius, r_0. The nondimensional hydrodynamic coefficients (denoted by overbars) take then the following form:

$$\bar{\kappa}_i = r_0\kappa_i, \quad \bar{\mu}_i = \frac{\mu_i}{\rho r_0^3}, \quad \bar{\lambda}_i = \frac{\lambda_i}{\rho r_0^3}, \quad \bar{\lambda}_{0i} = \frac{\lambda_{0i}}{\rho r_0^4}, \quad \bar{J}_0 = \frac{J_0}{\rho r_0^5}. \tag{31}$$

3. Modal equations for a tapered (truncated) conical tank

1. Natural sloshing modes and related hydrodynamic coefficients

Gavrilyuk *et al.* (2008) proposed two different sets of coordinate functions to get approximate natural sloshing modes, $\phi_i^{(m)}$, and frequencies by means of the global Trefftz method. Henceforth, we adopt the polynomial-type basis $\{w_k^{(m)}(x, r)\}$ from the paper by Gavrilyuk *et al.* (2008) and present the approximate natural sloshing modes as follows:

$$\phi_i^{(m)}(x, r) = \sum_{k=1}^{q} a_k^{(m,i)} w_k^{(m)}(x, r), \quad m = 0, 1, \ldots; \quad i = 1, 2, \ldots, \tag{32}$$

where q in the number of the polynomial-type coordinate functions and $a_k^{(m,i)}$ are the unknown coefficients. The Trefftz solution (32) satisfies the governing equation in the meridional cross-section G providing the fact that $\phi_i^{(m)}(x,r)cos(m\theta)$ and $\phi_i^{(m)}(x,r)sin(m\theta)$ are the harmonic functions.

Based on the Trefftz solution (32) (Gavrilyuk *et al.*, 2008), the approximate eigenvalues $\kappa_{m,i}$ and coefficients $a_k^{(m,i)}$ should be found from the spectral matrix problem:

$$\sum_{k,l=1}^{q} a_l^{(m,i)}\left(\alpha_{kl}^{(m,i)} - \kappa_{m,i}\gamma_{kl}^{(m,i)}\right) = 0, \tag{33}$$

where the matrix elements are defined by the formulas:

$$\alpha_{kl}^{(m)} = \int_{L_0+L_1+L_2} r\frac{\partial w_k^{(m)}}{\partial n} w_l^{(m)} ds; \quad \gamma_{kl}^{(m)} = \int_{L_0} r w_k^{(m)} w_l^{(m)} dr \tag{34}$$

(see geometric notations in Figure 1).

The spectral matrix problem (33) determines the eigenvectors:

$$\left(a_1^{(m,i)}, a_2^{(m,i)}, \ldots, a_q^{(m,i)}\right)$$

so that insertion of this vector into the Trefftz solution (32) gives the approximate natural modes $\phi_i^{(m)}(x,r)$ associated with $\kappa_{m,i}$. Because the natural sloshing modes are defined within to an arbitrary multiplier, one should impose a normalization. In the present paper, the normalization is provided by the condition:

$$\phi_i^{(m)}(0,r_0) = 1, \tag{35}$$

where r_0 is the radius of Σ_0. Using equation (35) is natural for the multimodal methods. Under this normalization, the generalized coordinates $\beta_i^c(t)$ and $\beta_i^s(t)$ play the role of the vertical wave elevation at the tank wall.

In terms of the Trefftz solution (32), the introduced normalization (35) implies that:

$$\left(a_1^{(m,i)}, a_2^{(m,i)}, \ldots, a_q^{(m,i)}\right)$$

should be scaled (divided) by:

$$N_{m,i} = \sum_{k=1}^{q} a_k^{(m,i)} w_k^{(m)}(0,r_0), \tag{36}$$

namely:

$$\bar{a}_k^{(m,i)} := \frac{a_k^{(m,i)}}{N_{m,i}}, \quad k = 1, \ldots, q; \quad \phi_i^{(m)}(x,r) = \sum_{k=1}^{q} \bar{a}_k^{(m,i)} w_k^{(m)}(x,r).$$

When postulating that the geometric dimensions are scaled by r_0 and using the aforementioned normalization, a simple algebra shows that the nondimensional hydrodynamic coefficients $\bar{\mu}_i$ and $\bar{\lambda}_i$ from Section 3 canbe calculated by the formulas:

$$\bar{\mu}_i = \frac{\pi\bar{\kappa}_{1,i}}{r_0^3}\sum_{k=1}^{q}\sum_{l=1}^{q}\bar{a}_k^{(1,i)}\bar{a}_l^{(1,i)}\gamma_{kl}, \qquad \bar{\lambda}_i = \frac{\pi\bar{\kappa}_{1,i}}{r_0^3}\sum_{k=1}^{q}\gamma_{1k}\bar{a}_k^{(1,i)}. \tag{37}$$

Our numerical experiments showed a fast stabilization of the significant figures for $\bar{\mu}_i$ and $\bar{\lambda}_i$ with increasing q in equation (32). Usually, $q = 20$ in the Trefftz solution (32) stabilizes five to six significant figures of the eigenvalues $\bar{\kappa}_i$ (see, also, convergence analysis by Gavrilyuk *et al.* (2008)), $\bar{\mu}_i$ and $\bar{\lambda}_i$.

2. Stokes-Joukowski potentials

A novelty with respect to the paper by Gavrilyuk *et al.* (2008) is that one must find the Stokes-Joukowski potentials, and, thereby, compute $\bar{J}_0$ and $\bar{\lambda}_{0i}$. This can be done by using the same harmonic basis of polynomial type employed in the Trefftz solution (32). For this purpose, we present an approximate solution of the problem (13) in the form:

$$\chi(x,r) = \sum_{k=1}^{q} b_k w_k^{(1)}(x,r) \tag{38}$$

(q is the number of coordinate functions) and note that the Neumann problem (13) is equivalent to minimizing the quadratic functional:

$$J(\chi) = \int_G \left(r\left(\frac{\partial\chi}{\partial x}\right)^2 + r\left(\frac{\partial\chi}{\partial x}\right)^2 + \frac{1}{r}\chi^2 \right) dS - 2\int_L r\chi g dS, \tag{39}$$

where $L = L_0 + L_1 + L_2$, and:

$$g = \begin{cases} r \text{ on } L_0, \\ -x\cos\theta_0 - r\sin\theta_0 \text{ on } L_1, \\ -r \text{ on } L_2. \end{cases} \tag{40}$$

By substituting equation (38) into functional (39) and using the necessary extrema condition:

$$\frac{\partial J(\chi)}{\partial b_k} = 0, \quad (k = 1, 2, \ldots, q), \tag{41}$$

we get the linear algebraic equations with respect to b_k :

$$\sum_{i,j=1}^{q} \alpha_{ij}^{(1)} b_j = \zeta_i^{(1)}, \tag{42}$$

where $\alpha_{ij}^{(1)}$ are defined by equation (34) and:

$$\zeta_i^{(1)} = \int_0^{r_0} \left(r^2 w_i^{(1)} \right)_{x=0} dr - \int_0^{r_1} \left(r^2 w_i^{(1)} \right)_{x=-h} dr$$

$$- \int_{-h}^{0} \left(r(x + r\tan\theta_0) w_i^{(1)} \right)_{r = x\tan\theta_0 + r_0} dx.$$

Introducing the scaling by r_0 and employing equations (38) and (42), we can find the remaining nondimensional hydrodynamic coefficients:

$$\bar{J}_0 = \frac{\pi}{r_0^5}\sum_{k=1}^{q} b_k \zeta_k^{(1)}, \quad \bar{\lambda}_{0i} = \frac{\pi\bar{\kappa}_{1,i}}{r_0^4}\sum_{k=1}^{q}\sum_{l=1}^{q}\gamma_{kl}\bar{a}_k^{(1,i)}b_l. \tag{43}$$

The Trefftz method demonstrates a faster convergence to $\bar{J}_0$ and $\bar{\lambda}_{0i}$ with increasing q in equation (38) than it has been in previous section for $\bar{\mu}_i$ and $\bar{\lambda}_i$. The same number q stabilizes, as a rule, one-two additional significant figures in $\bar{J}_0$ and $\bar{\lambda}_{0i}$.

3. Tables of nondimensional hydrodynamic coefficients

Dedicated calculations were done to table the nondimensional hydrodynamic coefficients versus the semiapex angle and $\bar{r}_1 = r_1/r_0$. Formulas (37) and (43) were used to get numerical values of the inertia tensor $\bar{J}_0$ as well as the hydrodynamic coefficients $\bar{\mu}_i$, $\bar{\lambda}_i$, and $\bar{\lambda}_{0i}$. The Trefftz method demonstrates different accuracy for different input parameters. This explains why Tables I-IV give the values with different accuracy, i.e. only stabilized significant figures (with $q = 20$) are included in the tables.

4. Validation

Convergence of the Trefftz method to eigenvalues $\bar{\kappa}_i$ was extensively investigated in the previous authors' paper (Gavrilyuk *et al.*, 2008). Two different sets of coordinate functions were used for a quality control. Numerical results by these two sets were compared to establish which of them provides a minimum error versus r_1/r_0, h/r_0, and θ_0.

Our numerical values of $\bar{\kappa}_i$ coincide with those by Gavrilyuk *et al.* (2005) who studied the limit case $\bar{r}_1 = 0$ (nontruncated conical tank). The numerical results by Gavrilyuk *et al.* (2005) were validated by experimental natural sloshing frequency $\sigma_1 = \sqrt{g\bar{\kappa}_1/r_0}$ from the papers by Mikishev and Dorozhkin (1961) and Bauer (1982) and,

$\bar{r}_1$	$\bar{J}_0$	$\bar{\kappa}_1$	$\bar{\kappa}_2$	$\bar{\kappa}_3$	$\bar{\kappa}_4$	$\bar{\kappa}_5$	$\bar{\kappa}_6$	$\bar{\kappa}_7$
				$\theta_0 = 30^\circ$				
0.0	0.517382	1.304395	4.922743	8.136674	11.30987	15.98363	20.0581	28.3418
0.2	0.487763	1.304377	4.922736	8.136621	11.30966	14.50351	18.4672	26.7118
0.4	0.380655	1.301685	4.921797	8.136589	11.30940	14.46874	17.5772	21.4216
0.6	0.276329	1.253965	4.906108	8.135757	11.30925	14.46827	17.6078	20.7919
0.8	0.184284	0.933815	4.739593	8.080329	11.29705	14.46603	17.6178	20.6563
				$\theta_0 = 45^\circ$				
0.0	0.175536	1.000000	4.483019	7.731563	10.91109	14.07253	17.2317	20.5515
0.2	0.171198	0.999553	4.482460	7.731550	10.91109	14.07253	17.2295	20.4839
0.4	0.159874	0.985702	4.465880	7.731183	10.91108	14.07252	17.2290	20.4407
0.6	0.145044	0.892940	4.371729	7.714013	10.90932	14.07228	17.2276	20.4253
0.8	0.105545	0.584313	3.855765	7.270504	10.68761	13.99165	17.2000	20.2425
				$\theta_0 = 60^\circ$				
0.0	0.090171	0.677680	3.621716	6.916305	10.11356	13.28055	16.4371	19.6142
0.2	0.089803	0.676232	3.617095	6.913924	10.11334	13.28054	16.4368	19.6025
0.4	0.088835	0.655289	3.557480	6.887986	10.10879	13.27960	16.4359	19.5647
0.6	0.083248	0.566042	3.366544	6.712571	10.01808	13.24914	16.4285	19.4858
0.8	0.060932	0.347496	2.669468	5.580759	8.931096	12.47492	15.9299	19.3281

Table I.
Nondimensional $\bar{J}_0$ and eigenvalues $\bar{\kappa}_i (i = 1, \ldots, 7)$

$\bar{r}_1$	$\bar{\mu}_1$	$\bar{\mu}_2$	$\bar{\mu}_3$	$\bar{\mu}_4$	$\bar{\mu}_5$	$\bar{\mu}_6$	$\bar{\mu}_7$
			$\theta_0 = 30^\circ$				
0.0	1.12237	4.9890	8.4272	11.9656	14.388	19.437	25.28
0.2	1.12236	4.9889	8.4190	11.7194	14.305	18.964	24.32
0.4	1.12113	4.9825	8.4113	11.7637	15.035	18.763	23.81
0.6	1.09833	4.8734	8.4074	11.7622	15.095	18.622	22.06
0.8	0.90121	4.4679	7.9889	11.6656	15.061	18.551	21.55
			$\theta_0 = 45^\circ$				
0.0	0.78540	3.2745	5.9642	8.4984	11.003	13.463	16.43
0.2	0.78523	3.2733	5.9640	8.4987	10.997	13.441	16.42
0.4	0.78098	3.2383	5.9591	8.4985	10.989	13.435	16.39
0.6	0.74680	3.0435	5.9148	8.4824	10.983	13.424	16.26
0.8	0.56645	2.9589	4.8744	7.8552	10.774	13.214	16.02
			$\theta_0 = 60^\circ$				
0.0	0.49801	1.79753	3.5197	5.2374	6.913	8.568	10.45
0.2	0.49771	1.79581	3.5146	5.2362	6.913	8.595	10.36
0.4	0.49301	1.76770	3.4560	5.2233	6.907	8.642	10.22
0.6	0.46482	1.66715	3.3546	4.9984	6.832	8.571	9.82
0.8	0.33850	1.84128	2.6135	4.2488	6.068	7.696	9.19

Table II.
Nondimensional hydrodynamic coefficients $\bar{\mu}_{1i} (i = 1, \ldots, 7)$

$\bar{r}_1$	$\bar{\lambda}_1$	$\bar{\lambda}_2$	$\bar{\lambda}_3$	$\bar{\lambda}_4$	$\bar{\lambda}_5$	$\bar{\lambda}_6$	$\bar{\lambda}_7$
			$\theta_0 = 30^\circ$				
0.0	1.07172	0.13840	0.06427	0.03673	0.0270	0.0077	0.0066
0.2	1.07170	0.13841	0.06431	0.03899	0.0271	0.0194	0.0068
0.4	1.06998	0.14024	0.06457	0.03924	0.0272	0.0206	0.0071
0.6	1.03912	0.17076	0.07025	0.04207	0.0289	0.0212	0.0168
0.8	0.81051	0.30826	0.12846	0.06711	0.0429	0.0307	0.0234
			$\theta_0 = 45^\circ$				
0.0	0.78540	0	0	0	0	0	0
0.2	0.78516	0.00049	−0.00007	0.00001	0.0000	0.0000	0.0000
0.4	0.77761	0.01514	−0.00180	0.00005	0.0000	0.0000	−0.0000
0.6	0.72338	0.09687	−0.00088	−0.00211	−0.0002	0.0001	0.0001
0.8	0.50812	0.24294	0.08866	0.02223	0.0019	−0.0020	−0.0015
			$\theta_0 = 60^\circ$				
0.0	0.51467	−0.05960	−0.00037	−0.00061	−0.0002	−0.0001	−0.0001
0.2	0.51397	−0.05755	−0.00179	−0.00021	−0.0003	−0.0001	−0.0001
0.4	0.50367	−0.02982	−0.01748	0.00187	0.0000	−0.0003	−0.0003
0.6	0.45432	0.05937	−0.03537	−0.01414	0.0004	0.0016	0.0002
0.8	0.30280	0.16554	0.05833	−0.00124	−0.0195	−0.0169	−0.0087

Table III.
Nondimensional hydrodynamic coefficients $\bar{\lambda}_i (i = 1, \ldots, 7)$

therefore, one can say that values $\bar{\kappa}_1$ with $\bar{r}_1 = 0$ in Table III are validated by comparison with experiments.

An additional validation of $\bar{\kappa}_i$ can be done by using experimental natural frequencies by El Damatty *et al.* (2000). In contrast to Mikishev and Dorozhkin (1961) and Bauer (1982), the model tests by El Damatty *et al.* (2000) were conducted for a truncated conical tank. The two lowest experimental natural frequencies by El Damatty *et al.* (2000) were $\nu_1^{exp} = 1.31\,\text{Hz}$ and $\nu_2^{exp} = 2.8\,\text{Hz}$ for a model tank with $\theta_0 = \pi/4$, $r_1 = 0.05\,\text{m}$,

$\bar{r}_1$	$\bar{\lambda}_{01}$	$\bar{\lambda}_{02}$	$\bar{\lambda}_{03}$	$\bar{\lambda}_{04}$	$\bar{\lambda}_{05}$	$\bar{\lambda}_{06}$	$\bar{\lambda}_{07}$
				$\theta_0 = 30^\circ$			
0.0	0.60859	−0.15537	−0.08771	−0.05762	−0.0424	−0.0124	−0.0113
0.2	0.60841	−0.15525	−0.08757	−0.05714	−0.0408	−0.0303	−0.0163
0.4	0.59852	−0.14831	−0.08641	−0.05361	−0.0405	−0.0323	−0.0107
0.6	0.51675	−0.08966	−0.07462	−0.05061	−0.0369	−0.0266	−0.0227
0.8	0.25285	0.04294	−0.01615	−0.02484	−0.0221	−0.0181	−0.0158
				$\theta_0 = 45^\circ$			
0.0	0.31416	−0.14873	−0.04966	−0.02531	−0.01535	−0.0103	−0.0075
0.2	0.31329	−0.14765	−0.04983	−0.02530	−0.01535	−0.0102	−0.0077
0.4	0.29689	−0.12663	−0.05254	−0.02523	−0.01533	−0.0102	−0.0079
0.6	0.22919	−0.04966	−0.05190	−0.02747	−0.01554	−0.0102	−0.0075
0.8	0.09420	0.02802	−0.00607	−0.01610	−0.01509	−0.0115	−0.0082
				$\theta_0 = 60^\circ$			
0.0	0.13197	−0.08677	−0.00059	−0.00100	−0.0003	−0.0002	−0.0001
0.2	0.13086	−0.08481	−0.00209	−0.00057	−0.0004	−0.0002	−0.0002
0.4	0.11963	−0.06472	−0.01476	0.00118	−0.0002	−0.0003	−0.0002
0.6	0.08646	−0.01878	−0.02641	−0.00773	0.0002	0.0007	0.0001
0.8	0.03277	0.01268	−0.00168	−0.00790	−0.0077	−0.0051	−0.0024

Table IV. Nondimensional hydrodynamic coefficients $\bar{\lambda}_{0i} (i = 1, \ldots, 7)$

and liquid depth $h = 0.1$ m. According to our Trefftz method, these frequencies are $\nu_1 = \sqrt{g\bar{\kappa}_1/r_0}/(2\pi) = 1.28$ Hz and $\nu_2 = \sqrt{g\bar{\kappa}_2/r_0}/(2\pi) = 2.72$ Hz, respectively. The difference is less than 3 percent that is, we believe, due to the surface tension which is, generally, not negligible for the relatively-small model tank by El Damatty *et al.* (2000) (see, Section 4.2 by Faltinsen and Timokha (2009)).

To validate numerical results on the Stokes-Joukowski potentials, we can compare our values of $\bar{J}_0$ with earlier calculations by Lukovsky *et al.* (1984) and Shvets (1988). The latter calculations were done for nontruncated conical tanks ($\bar{r}_1 = 0$) with $\theta_0 = \pi/6, \pi/4$, and $\pi/3$. The three values of $\bar{J}_0$ in the first column of Table III (corresponding to $\bar{r}_1 = 0$) have the same four significant figures as those in the papers by Lukovsky *et al.* (1984) and Shvets (1988).

Finally, we can validate $\bar{\lambda}_i$ and $\bar{\mu}_i$ by using model tests by Casciati *et al.* (2003). Casciati *et al.* (2003)'s experimental setup consists of a rigid load cell containing a rigid tapered conical tank with $\theta_0 = \pi/6$ and $r_1 = 0.1$ m; the tank is partially filled with a liquid with different liquid depths. The setup is installed on a shaking table performing the horizontal harmonic motions $\eta_2(t) = \eta_{2a} cos(\sigma t)$ where σ is the forcing frequency and η_{2a} is the forcing amplitude. Casciati *et al.* (2003) focus on the steady-state force caused by the setup harmonic motions. This force is the sum of the inertia force due to the rigid tank and load cell and the steady-state hydrodynamic force due to sloshing. The experimental results are presented in a nondimensional form appearing as the transfer function $F_{2a}/(M_l \eta_{2a} \sigma^2)$ for the force amplitude F_{2a}. Using our linear modal equations (18) and formula (25) with $\eta_2(t) = \eta_{2a} cos(\sigma t)$, we can find the steady-state hydrodynamic force and estimate this transfer function as:

$$\frac{F_{2a}}{M_l \eta_{2a} \sigma^2} = 1 + \frac{M_{cell}}{M_l} + \frac{r_0^3}{V_l} \sum_{k=1}^{q_1} \frac{\bar{\lambda}_k \sigma^2}{\bar{\mu}_k \left(\sigma_k^2 - \sigma\right)}, \tag{44}$$

where V_l is the liquid volume, $M_l = \rho V_l$ is the liquid mass, q_1 is the number of the used modal equations, and M_{cell} is the total mass of the load cell and the rigid tank ($M_l = 10.5$ kg in the model tests by Casciati *et al.* (2003)).

Comparison of experimental values by Casciati *et al.* (2003) and those by formula (44) is shown in Figure 3. In formula (44), seven significant figures of the transfer function stabilize with $q_1 = 5$ for input parameters associated with (Casciati *et al.*, 2003). The theoretical results are marked by the solid lines. Because we have constructed a *linear* theory, these

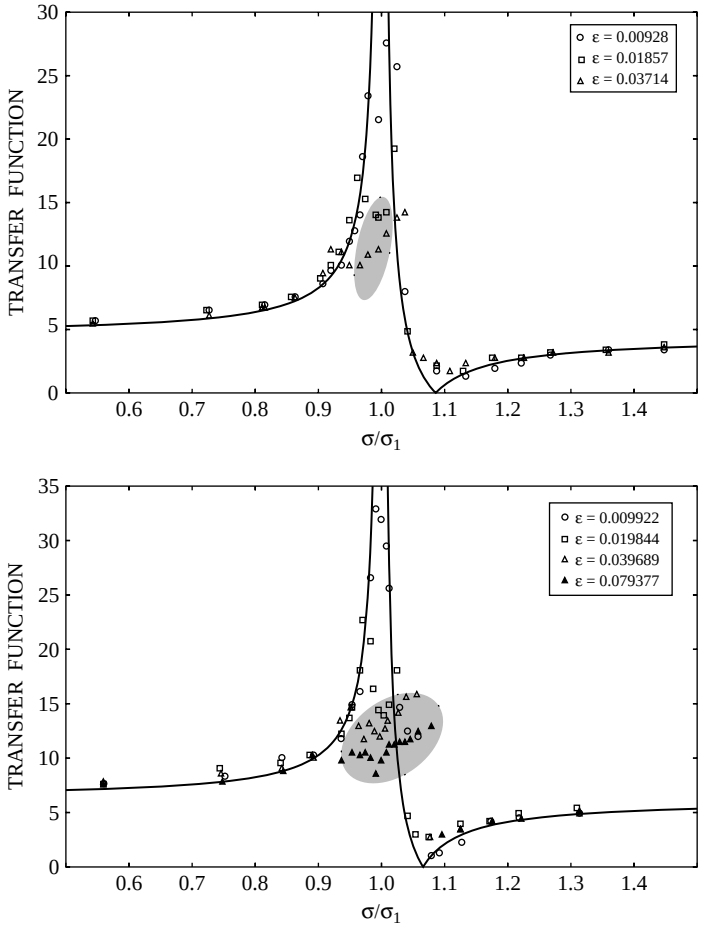

Notes: Our linear modal theory (solid line) predicts this transfer function by formula (44); the model tests were conducted with different nondimensional forcing amplitudes $\varepsilon = \eta_{2a}/r_0$; theoretical results do not depend on 1, but experimental values can depend on ε due to the free-surface nonlinearity; the shadow zone marks the experimental points for which the free-surface nonlinearity is important; the case (a) is for $h/(2r_0) = 0.228$, the case (b) deals with $h/(2r_0) = 0.1786$

Figure 3.
The transfer function for the steady-state force amplitude $(F_{2a}/(\eta_{2a}M_l\sigma^2))$ associated with model tests by Casciati *et al.* (2003)

theoretical results do not depend on the nondimensional forcing amplitude $\varepsilon = \eta_{2a}/r_0$. However, experimental force amplitudes can change with ε in a neighborhood of $\sigma/\sigma_1 = 1$ when sloshing becomes of resonant nature and, therefore, strongly nonlinear. The free-surface nonlinearity is more important for larger ε and smaller liquid depth $h/(2r_0)$. These facts are clearly seen in Figure 3.

Figure 3(a) deals with the largest experimental liquid depth $h/(2r_0) = 0.228$. Here, the experimental transfer function displays the free-surface nonlinearity in the frequency range $0.95 < \sigma/\sigma_1 < 1.05$ (see, the shadow zone). Formula (44) gives a good prediction of the experimental values outside of this range. Moreover, theoretical results agree with experimental values for the lowest forcing amplitude $\varepsilon = \eta_{2a}/r_0 = 0.00928$ except for one measurement point at $\sigma/\sigma_1 = 1$ where our linear theory leads to infinite force amplitude but the experiments do not support that.

The experimental points in Figure 3(b) are for the lower liquid depth $h/(2r_0) = 0.1786$ which, generally, belongs to the so-called intermediate liquid depths whose range was roughly estimated by Faltinsen and Timokha (2002) as $0.1 \lesssim h/(2r_0) \lesssim 0.2$. The linear sloshing theory is weakly applicable for the intermediate liquid depths. Figure 3(b) shows that the free-surface nonlinearity becomes important in the resonance frequency range $0.9 < \sigma/\sigma_1 < 1.1$ (see, shadow zone). Away from this range, our linear modal theory is supported by the model tests. Moreover, the theory gives also satisfactory agreement in the range $0.9 < \sigma/\sigma_1 < 1.1$ for the lowest experimental forcing amplitude $\eta_{2a}/r_0 = 0.009922$ when the free-surface nonlinearity is less important than for the larger experimental forcing amplitudes $\eta_{2a}/r_0 = 0.019844, 0.039689$, and 0.079377.

4. Coupled "tank-external structure" dynamics

Using the derived linear modal equations in simulating the liquid sloshing for prescribed motions of the rigid tapered conical tank looks now a rather simple task. The simulations reduce to the Runge-Kutta integration of the ODEs (17).

Describing the coupled dynamics of the rigid tank and an external structure assumes that we can incorporate modal equations (17) into global dynamic equations taking into account that we know expressions for the resulting sloshing force and moment in terms of the generalized coordinates β_i^c and β_i^s. The corresponding procedure will furthermore be exemplified for two mechanical systems.

1. Sretenski's problem (dynamic damper)

Let us consider Sretenski's (1951) mechanical system in Figure 4. It consists of a rigid platform of the mass M_p, a rigid tank partly filled with the tank, and a spring (linked to a rigid wall) with the Hooke coefficient k. The platform can move horizontally without friction. The rigid conical tank of the mass M_t is installed on the platform. The Sretenski problem consists of describing the small oscillatory motions of the platform (relative to its static equilibrium position), that is, the sloshing-structure system, exposed to an external forcing F(t).

1. The global dynamics and modal equations. Because the platform moves with a single degree of freedom (here, the translatory motions along the Oz-axis) and $\eta_1 = \eta_2 = \eta_4 = \eta_5 = \eta_6 = 0$, the platform displacements can be associated with the generalized coordinate $\eta_3(t)$. Assuming that $\eta_3(t)$ is known, we can describe the linear forced sloshing by using the modal system (19) with the right-hand side proportional to $\ddot{\eta}_3$:

$$\mu_i(\ddot{\beta}_i^s + \sigma_i^2\beta_i^s) = -\lambda_i\ddot{\eta}_3, \quad i = 1, 2, \ldots \tag{45}$$

The horizontal hydrodynamic force along the *Oz*-axis is, according to formula (26):

$$F_3(t) = -M_l\ddot{\eta}_3 - \sum_{k=1}^{\infty}\ddot{\beta}_k^s\lambda_k. \tag{46}$$

Equations (45) and (46) show that the resulting hydrodynamic force is a function of η_3 and β_i^s. This force gives rise in the global dynamic equation (Newton' law) of the platform which takes the form:

$$(M_t + M_p)\ddot{\eta}_3 = -k\eta_3 + F_3 + \mathrm{F}. \tag{47}$$

The global dynamic equation (47) accounts for the resulting horizontal forces acting on the rigid body of the total mass $M_t + M_p$ including the external forcing F(t), the spring resistance force $-k\eta_3$, and the hydrodynamic force $F_3(t)$. Inserting the hydrodynamic force equation (46) into equation (47) leads to:

$$M_0(\ddot{\eta}_3 + \sigma_0^2\eta_3) + \sum_{k=1}^{\infty}\ddot{\beta}_k^s\lambda_k = \mathrm{F}, \tag{48}$$

where $M_0 = M_t + M_p + M_l$ is the total mass and $\sigma_0 = \sqrt{k/M_0}$ is the natural frequency of the spring-mass platform oscillations with a "frozen" liquid inside.

In summary, to describe the platform-sloshing interaction with a known external forcing F(t), we should solve the system of ODEs (48) and (45). Equation (48) is responsible for the platform displacements, and modal equations (45) describe sloshing. The appropriate nondimensional hydrodynamic coefficients can be taken from Tables I-IV.

2. Steady-state motions and dynamic liquid damper. We consider the harmonic external force F= $\eta_a M_0\sigma^2 cos(\sigma t)$ where η_a is the acceleration amplitude, and σ is the forcing frequency. Our task consists of describing the steady-state motions of the Sretenski system. In terms of the dynamic equations (48) and (45), the steady-state motions are associated with the harmonic solution:

$$\beta_i = A_i\cos(\sigma t), \quad \eta_3 = B\cos(\sigma t), \tag{49}$$

where B is the steady-state amplitude of the platform motions, and A_i are amplitudes of the sloshing-related generalized coordinates. Substituting equation (49) into equations (48) and (45) gives:

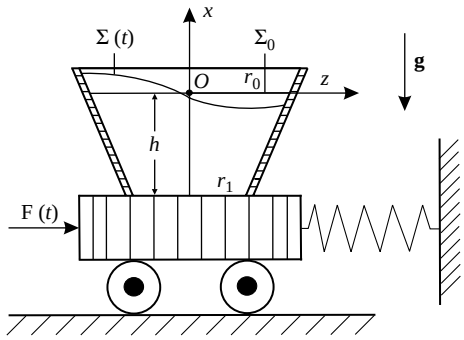

Figure 4.
Sketch of a mobile platform with a conical tank installed on the platform

$$\bar{B} = \frac{B}{\eta_a} = \left((\bar{\sigma}_0^2 - 1) - \frac{\rho r_0^3}{M_0} - \sum_{i=1}^{\infty} \frac{\bar{\lambda}_i^2}{\bar{\mu}_i (\bar{\sigma}_i^2 - 1)} \right)^{-1}, \tag{50}$$

where $\bar{\sigma}_0 = \sigma_0/\sigma$ and $\bar{\sigma}_i = \sigma_i/\sigma$.

Analyzing expression (50), we can study dependence of the nondimensional steady-state platform amplitude on various input parameters. A particular interest is dependence of the nondimensional amplitude on the forcing frequency for the case $\sigma_0 = \sigma_1$, namely, when the eigenfrequency of the whole mechanical system with "frozen" liquid coincides with the lowest natural sloshing frequency. By detuning σ_1 to be equal to σ_0, the wave tank can play the role of the so-called dynamic liquid damper.

Results of numerical experiments are shown in Figure 5. Seven modal equations of (45) are used providing, as our numerical tests showed, stabilization of three-four significant figures of the $\bar{B}$-value for the semiapex angles $\theta_0 = 30^\circ, 45^\circ$ and 60°, $r_1 = 0.4$, and $\rho r_0^3/M_0 = 0.5$. The graphs in Figure 5 demonstrate that, when $\sigma = \sigma_0 = \sigma_1$, the platform remains immobile in steady-state conditions. Thus, sloshing really "works" as a dynamic damper, i.e. the resulting hydrodynamic force due to sloshing counteracts the external force F(t) preventing any platform displacements. However, we see a resonance point for $\sigma/\sigma_0 < 1$ as well as there are higher resonance frequencies associated with higher natural sloshing frequencies.

2. Water tower with an elevated conical tank

The next example is the mechanical system consisting of a tower with a conical elevated tank on the top. Schematically, this mechanical system is shown in Figure 6. In the forthcoming analysis, we assume, that the tank mass M_t is negligible with respect to the liquid mass M_l, i.e. $M_t \ll M_l$. Besides, we assume that the tower performs transverse

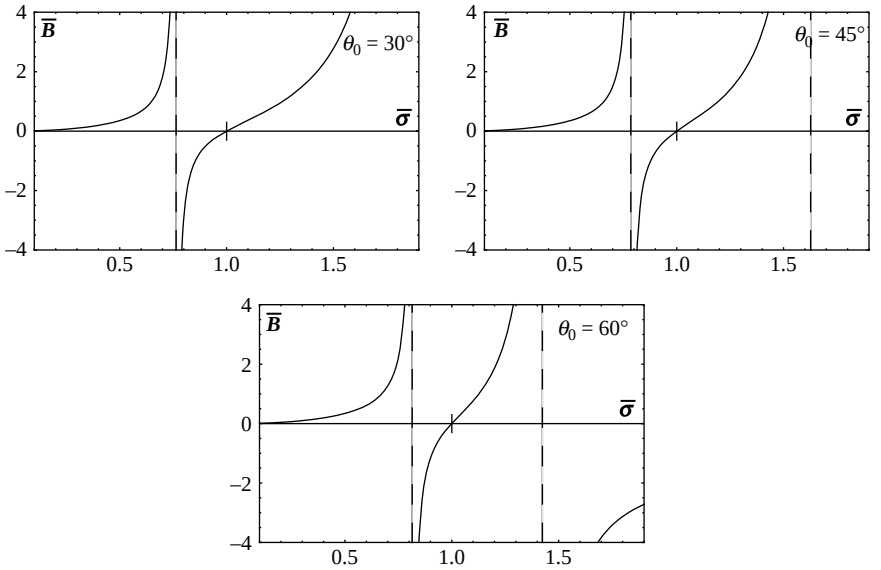

Figure 5.
The nondimensional steady-state platform amplitude as a function of $\bar{\sigma} = \sigma/\sigma_0$

Notes: In the numerical example, $\sigma_0 = \sigma_1$, $\rho r_0^3/M_0 = 0.5$ and $r_1 = 0.4$

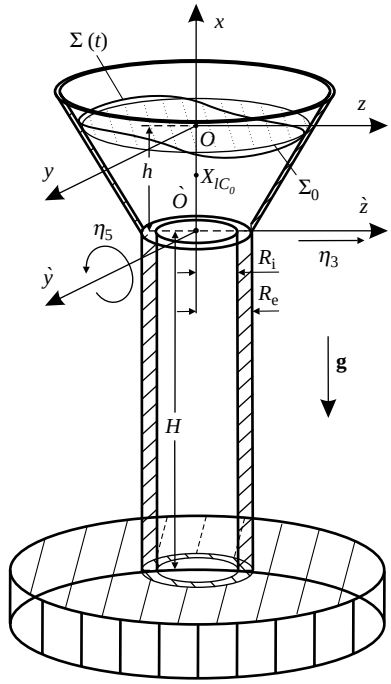

Figure 6.
Sketch of a water tower with a conical tank

vibrational motions, and neglect vertical compression of the tower due to the liquid weight. For brevity, the tower motions are considered in the *Oxz*-plane. These are modeled by Euler's beam. The tower height (Euler's beam length) is denoted by H, the outer tower radius coincides with the tank bottom radius, $R_e = r_1$, and the inner tower radius (shaft radius) is equal to $R_i = k_i r_1$, where nondimensional factors k_i $(0 < k_i < 1)$ are introduced to match specific properties of the tower. The water tower motions are described in the coordinate system $Ò\dot{x}\dot{y}\dot{z}$ whose origin coincides with the tank bottom center in its static position.

1. The beam equation and boundary conditions at the earth-fixed beam end. The beam oscillations are modeled by the Euler-Bernoulli equation:

$$m_b \ddot{W} + (EIW'')'' = 0, \tag{51}$$

where function $W(x,t)$ describes the beam deviation in the $Òxz$-plane, E is Young's modulus, I is the second moment of inertia (being equal to $I = (1/4)\pi(R_e^4 - R_i^4)$), $m_b = \pi\rho_c(R_e^2 - R_i^2)$ is the linear beam mass (mass per unit length), and ρ_c is the material density. The prime denotes the spatial differentiation by x.

The clamped-end boundary conditions at the Earth-fixed end are expressed as:

$$W(-H,t) = 0, \quad W'(-H,t) = 0. \tag{52}$$

2. Boundary conditions on the beam top. These conditions should express equivalence between the bending moment and force of the beam and the hydrodynamic moment

and force due to sloshing (as we said, we neglect the tank mass), respectively, i.e.:

$$EIW''(0,t) = -F_5^{\grave{O}}; \quad (EIW'')'(0,t) = -F_3^{\grave{O}}, \tag{53}$$

where $F_3^{\grave{O}}(t)$ is the horizontal hydrodynamic force along the $\grave{O}\grave{x}\grave{y}\grave{z}$-axis, and $F_5^{\grave{O}}(t)$ is the hydrodynamic moment around the $O\grave{y}$-axis.

The hydrodynamic force $F_3^{\grave{O}}(t)$ and moment $F_5^{\grave{O}}(t)$ are perturbed by the beam top oscillations associated with the horizontal displacement $u(t)$ along the $\grave{O}z$-axis, and inclination $\theta_1(t)$ around the $\grave{O}y$-axis which are, by definition:

$$u = W(0,t), \quad \theta_1 = -W'(0,t). \tag{54}$$

The hydrodynamic force and moment can be expressed in terms of the generalized coordinates appearing in the modal equations. We should take into account that the origin $Oxyz$ does not belong to the mean liquid surface (as it has been accepted in Sections 2 and 3). According to definitions in Section 2, we should link u, θ_1 and η_3, η_5 by the following relations:

$$\eta_5 = \theta_1, \quad \eta_3 = u - h\theta_1,$$

and substitute η_3 and η_5 into original boundary value problem (1), modal equations (19), and formulas for the hydrodynamic force and moment, (26) and (28), respectively.

Following the formulas (26) (in projections on the coordinate system $\grave{O}\grave{x}\grave{y}\grave{z}$), equations (28) and (30) (related to the point $A = \grave{O}$), the corresponding hydrodynamic force and moment in equation (53) can be derived in the form:

$$F_3^{\grave{O}} = M_l(\theta_1 X_{lC_0} - \ddot{u}) - \sum_{k=1}^{\infty} \ddot{\beta}_k^s \lambda_k, \tag{55}$$

$$F_5^{\grave{O}} = M_l X_{lC_0}(g\theta_1 + \ddot{u}) - J_0\theta_1 - \sum_{j=1}^{\infty} \left(-\lambda_{0j}\ddot{\beta}_j^s + g\lambda_j\beta_j^s\right), \tag{56}$$

where X_{lC_0} is the vertical coordinate of the liquid mass center in the $\grave{O}\grave{x}\grave{y}\grave{z}$-system, $J_0 = M_l h(2X_{lC_0} - h) + J_0$, $\lambda_{0i}^O = \lambda_{0i} + h\lambda_i$, and the generalized coordinates β_j^s are the solution of the ODEs (19). The latter can be rewritten as follows:

$$\mu_i\left(\ddot{\beta}_i^s + \sigma_i^2\beta_i^s\right) = -\lambda_i(\ddot{u} + g\theta_1) + \lambda_{0i}\theta_1. \tag{57}$$

3. Coupled eigenoscillations. We consider eigenoscillations of the whole mechanical system, i.e.:

$$W(x,t) = \mathscr{W}(x)cos\sigma t, \quad \beta_i^s(t) = B_i cos\sigma t, \tag{58}$$

where σ is the eigenfrequency; variables B_i and function $\mathscr{W}(x)$ determine the steady-state modal sloshing amplitudes and the beam eigenmode for the coupled eigenmotions. Substituting equation (58) into modal equations (57) gives:

$$B_i = \frac{\sigma^2}{\mu_i(\sigma_i^2 - \sigma^2)}\left[\lambda_i\mathscr{W}(0) + \left(\frac{\lambda_i g}{\sigma^2} + \lambda_{0i}\right)\mathscr{W}'(0)\right], \tag{59}$$

and, thereby, we can derive the modified boundary conditions at the beam top in terms of the eigenmode $\mathscr{W}(x)$. The sloshing-modified eigenoscillations of the tower are therefore described by nontrivial solutions of the following homogeneous problem:

$$-\sigma^2 m_b \mathscr{W} + (EI\mathscr{W}'')'' = 0, \quad x \in [-H, 0], \tag{60}$$

$$\mathscr{W}(-H) = \mathscr{W}'(-H) = 0, \tag{61}$$

$$EI\mathscr{W}''(0) = \sigma^2[A_1\mathscr{W}(0) + A_3\mathscr{W}'(0)], \tag{62}$$

$$(EI\mathscr{W}'')'(0) = -\sigma^2[A_2\mathscr{W}(0) + A_1\mathscr{W}'(0)], \tag{63}$$

with respect to function $\mathscr{W}(x)$ and spectral parameter σ^2. The coefficients $A_1(\sigma^2)$, $A_2(\sigma^2)$, and $A_3(\sigma^2)$ depend on σ^2 and take the form:

$$\begin{aligned} A_1 &= M_l X_{lC_0} + \sum_{j=1}^{\infty} \frac{\lambda_j(\lambda_{oj} + \lambda_j g/\sigma^2)}{\mu_j(\bar{\sigma}_j^2 - 1)}, \\ \mathrm{A}_2 &= M_l + \sum_{j=1}^{\infty} \frac{\lambda_j^2}{\mu_i(\bar{\sigma}_j^2 - 1)}, \quad A_3 = \frac{M_l X_{lC_0} g}{\sigma^2} + J_0 + \sum_{j=1}^{\infty} \frac{(\lambda_{0j} + \lambda_j g/\sigma^2)^2}{\mu_j(\sigma_j^2 - 1)}. \end{aligned} \tag{64}$$

The nonlinear spectral problem (59) admits variational formulation associating the eigenmodes with local extrema of the quadratic functional:

$$F(\mathscr{W}) = \int_{-H}^{0} \left[\sigma^2 m_b \mathscr{W} - (EI\mathscr{W}'')^2\right] dx + \sigma^2[A_2\mathscr{W}^2 + A_3(\mathscr{W}')^2 + 2A_1\mathscr{W}\mathscr{W}']_{x=0} \tag{65}$$

restricted to kinematic conditions (61). This fact makes it possible to use variational methods.

Galerkin's variational method expresses $\mathscr{W}(x)$ in the form:

$$\mathscr{W} = \sum_{k=1}^{q} a_k \psi_k, \tag{66}$$

where each function $\psi_k(x)$ satisfies boundary conditions (61). Using the necessary extrema condition of functional (65), we associate the eigenfrequencies with zeros of the determinant:

$$D(\sigma) = \det|\{e_{ij}\} - \sigma^2\{f_{ij}\}| = 0, \tag{67}$$

where the matrix elements are given by the formulas:

$$\begin{aligned} e_{ij} &= \textstyle\int_{-H}^{0} EI\psi_i''\psi_j'' dx, \\ f_{ij} &= \textstyle\int_{-H}^{0} m_b\psi_i\psi_j dx + \left[A_2(\sigma^2)\psi_i\psi_j + A_3(\sigma^2)\psi_i'\psi_j' + A_1(\sigma^2)(\psi_i\psi_j' + \psi_i'\psi_j)\right]_{x=0}. \end{aligned}$$

A simplest set of coordinate functions in representation (66) can be the polynomials:

$$\psi_k = \frac{\hat{\psi}_k}{N_k}, \quad \hat{\psi}_k(x) = (x+H)^{(k+1)}, \quad N_k = \sqrt{\int_{-H}^{0} \hat{\psi}_k^2(x)dx}.$$

4. Numerical experiments. In our numerical experiments, an emphasis is placed on the case when the lowest natural sloshing frequency, σ_1, coincides with the first structural eigenfrequency, σ_{01}. The latter frequency is associated with eigenoscillations of the mechanical system in which the liquid free surface does not move, namely, it is covered by an artificial rigid roof. This eigenfrequency can be found by our variational method where the liquid sloshing amplitudes are zero, i.e. $B_i = 0$ in equation (59).

Choosing, for example, $\bar{r}_1 = \bar{R}_b = 0.4$ and $\theta_0 = \pi/4$, one can vary R_b/H_b, k_b, k_i $(0 < k_i < 1, k_b > 1)$, $H_b = H = k_b r_1, R_i = k_i r_1$, to find suitable values of physical and geometrical values which provide equivalence of σ_1 and σ_{01}. The equality $\sigma_1 = \sigma_{01}$ is, for instance, fulfilled with $k_i = 0.7$ and $k_b = 28.15$ which correspond to the geometrical structural parameters: the free-surface diameter is equal to 2.5 m, the liquid depth is equal to 1.5 m, the beam diameter is equal to 1 m, and the beam length is equal to 28.15 m. The liquid is a fresh water with $\rho_l = 1.0 \cdot 10^3$ kg/m^3, and the tower body is the reinforced concrete, $\rho_c = 2.4 \cdot 10^3$ kg/m^3 whose Young's modulus is $E = 6 \cdot 10^6$ N/m^2. Figure 7 shows the graph of $D(\sigma)$ (equation (67)) computed with these input parameters. The $\sigma_1 = \sigma_{01}$-value is denoted as "sloshing". The graph shows that this partial eigenfrequency splits into the two different eigenfrequencies, "coupled 1" and "coupled 2" demonstrated in Figure 7.

5. Concluding remarks

The linear multimodal method was developed for the case of a tapered conical tank. We assume decoupling of the hydrodynamic loads and elastic tank vibrations which is, for instance, possible when the elastic tank vibrations have eigenfrequencies that are much higher than the lowest natural sloshing frequency. The rigid tank can perform small-magnitude oscillatory motions and be a part of a complex mechanical system, e.g. storage (elevated) tank. Approximate natural sloshing modes and Stokes-Joukowski's potentials were constructed. The approximate natural sloshing modes were obtained by using the Trefftz variational method proposed by Gavrilyuk *et al.* (2008). It was found that the same method can be implemented for

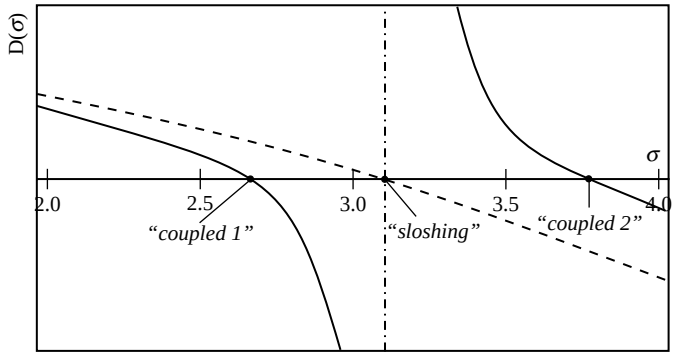

Figure 7.
Determinant $D(\sigma)$ as a function of σ

finding the Stokes-Joukowski potentials. Based on the approximate Trefftz solutions, we computed the hydrodynamic coefficients of the linear modal equations that couple generalized coordinates responsible for displacements of the natural sloshing modes. In the right-hand side, the latter equations contain six generalized coordinates responsible for translatory and angular motions of the rigid tank.

Using the linear modal equations simplifies description of the coupled dynamics of complex mechanical systems containing a tapered conical tank partially filled with a liquid. The coupling involves expressions for the resulting hydrodynamic (sloshing) force and moment. The force and moment are basically determined by "dynamic" sloshing loads. In the present paper, we show how to use the Lukovsky formulas to get "modal" expressions for these force and moment. The modal expressions give the force and moment as a linear function of the generalized coordinates and their time-derivatives. These expressions use the same hydrodynamic coefficients as in the derived linear modal equations. The coefficients (in nondimensional form) are computed and tabled. Employing these tables helps practically oriented readers who want to use the linear modal equations. The corresponding models can be considered as an alternative to the CFD and equivalent mechanical systems. The numerical hydrodynamic coefficients were validated by comparing with earlier computations and experimental data.

Abilities of these "modal" models are exemplified for two test problems. The first problem is on the dynamic damper containing the tapered conical tank (Sretenski's problem). It has been demonstrated that the multimodal method requires only several relatively simple linear ODEs for description of the carrying platform motions. The second problem is on the coupled eigenoscillations of a water tower with an elevated conical tank.

References

Bauer, H.F. (1982), "Sloshing in conical tanks", *Acta Mechanica*, Vol. 43 Nos 3/4, pp. 185-200.

Casciati, F., De Stefano, A. and Matta, E. (2003), "Simulating a conical tuned liquid damper", *Simulation Modelling Practice and Theory*, Vol. 11, pp. 353-70.

Dokuchaev, L.V. (1964), "On the solution of a boundary value problem on the sloshing of a liquid in conical cavities", *Applied Mathematics and Mechanics* (*PMM*), Vol. 28, pp. 151-4.

Dutta, S., Mandal, A. and Dutta, S.C. (2004), "Soil-structure interaction in dynamic behaviour of elevated tanks with alternate frame staging configurations", *Journal of Sound and Vibration*, Vol. 277, pp. 825-53.

El Damatty, A. and Sweedan, A.M.I. (2006), "Equivalent mechanical analog for dynamic analysis of pure conical tanks", *Thin-Walled Structures*, Vol. 44, pp. 429-40.

El Damatty, A., Korol, R.M. and Tang, L.M. (2000), "Analytical and experimental investigation of the dynamic response of liquid-filled conical tanks", *Proceedings of the World Conference of Earthquake Engineering, New Zealand*, Paper No. 966, Topic No. 7, pp. 1-8.

El Damatty, A., Saafan, M.S. and Sweedan, A.M.I. (2005), "Experimental study conducted on a liquid-filled combined conical tank model", *Thin-Walled Structures*, Vol. 43, pp. 1398-417.

Faltinsen, O.M. and Timokha, A.N. (2002), "Asymptotic modal approximation of nonlinear resonant sloshing in a rectangular tank with small fluid depth", *Journal of Fluid Mechanics*, Vol. 470, pp. 319-57.

Faltinsen, O.M. and Timokha, A.N. (2009), *Sloshing*, Cambridge University Press, Cambridge, MA.

Gavrilyuk, I., Lukovsky, I. and Timokha, A. (2005), "Linear and nonlinear sloshing in a circular conical tank", *Fluid Dynamics Research*, Vol. 37, pp. 399-429.

Gavrilyuk, I., Hermann, M., Lukovsky, I., Solodun, O. and Timokha, A. (2008), "Natural sloshing frequencies in rigid truncated conical tanks", *Engineering Computations*, Vol. 25 No. 6, pp. 518-40.

Joukowski, N. (1885), "On motions of a rigid body with cavity filled by homogeneous liquid", *Journal of Russian Physical-Mathematical Society*, Vol. XVI, pp. 30-85.

Lukovsky, I.A. (1990), *Introduction to Nonlinear Dynamics of Rigid Bodies with the Cavities Partially Filled by a Fluid*, Naukova Dumka, Kiev.

Lukovsky, I.A. and Timokha, A.N. (1995), *Variational Methods in Nonlinear Dynamics of a Limited Liquid Volume*, Institute of Mathematics of NASU, Kiev.

Lukovsky, I.A., Barnyak, M.Ya. and Komarenko, A.N. (1984), *Approximate Methods of Solving of Dynamics Problem of the Limited Volume of Fluid*, Naukova Dumka, Kiev.

Lukovsky, I.A., Trotsenko, V.A. and Feschenko, S.F. (1984), *Calculation of Dynamic Characteristics of a Liquid in Mobile Cavities*, Academy of Sciences of UkrSSR, Kiev.

Mikishev, G.N. and Dorozhkin, N.Y. (1961), "An experimental investigation of free oscillations of a liquid in containers", *Izvestiya Akademii Nauk SSSR. Otdelenie Tekhnicheskikh Nauk: Mekhanika, Mashinostroenie*, No. 4, pp. 48-53 (in Russian).

Morand, J.-P. and Ohayon, R. (1995), *Fluid Structure Interaction: Applied Numerical Methods*, Wiley, Chichester.

Shvets, G.A. (1988), *Determining the Dynamic Characteristics of a Rigid Body with Non-symmetric Cavities*, Academy of Sciences of UkrSSR, Institute of Mathematics, Kiev.

Sretenski, L.N. (1951), "Oscillations of a liquid in a container", *Izvsetiya AN SSSR. Otdeleniye Techn. Nauk*, No. 10, pp. 1483-94.

Sweedan, A.M.I. (2009), "Equivalent mechanical model for seismic forces in combined tanks subjected to vertical earthquake excitation", *Thin-Walled Structures*, Vol. 47, pp. 942-52.

Corresponding author
Alexander Timokha can be contacted at: alexander.timokha@ntnu.no